Impact of fiber loss on two-soliton states: Substantial changes in eigenvalue spectrum

Alexander Hause, Christoph Mahnke, and Fedor Mitschke[*]

Universität Rostock, Institut für Physik, 18051 Rostock, Germany

The impact of power loss on fiber-optic solitons and soliton compounds has regained interest recently, as coding schemes employing inverse scattering eigenvalues are being discussed. Loss lifts the integrability of the underlying nonlinear Schrödinger equation and has usually been treated by perturbation analysis. Our approach uses localized loss of arbitrary strength. We investigate two-soliton compounds including the $N = 2$ soliton and show that loss causes severe qualitative modifications of the eigenvalue spectrum. Peculiar features include power redistribution between solitons so that one of them is actually enhanced by loss and conversion of solitons at rest into a pair with outward velocities. Earlier reports of such features are put into context. We argue that frequency splitting of soliton pairs requires a mechanism that renders the spectrum double-lobed (or multiply lobed) and that the bifurcation is defined by a balance between dispersive and nonlinear forces. Implications for eigenvalue-based communication formats are pointed out.

I. INTRODUCTION

Optical transmission of telecommunication signals is enormously successful and carries the bulk of worldwide data traffic. However, due to relentless growth of traffic volume, the data-carrying capacity of fibers is already pushed to the limits [1]. Fiber production and deployment cannot keep up with rising demand. All degrees of freedom in coding (wavelength, polarization, amplitude, and phase multiplexing) available in a linear system are exhausted. Some authors suggest using spatial degrees of freedom [2], but those require specialty fibers. In this situation another look into nonlinear transmission schemes is warranted; while those have their own challenges, to increase signal amplitudes seems to be the only way to go. Fortunately, the soliton concept is quite robust [3], and its extension to soliton molecules [4,5] demonstrates that it is not restricted to the inefficient binary transmission (on-off keying) format.

A central challenge to assess solitonic transmission systems is that while the underlying equation, the nonlinear Schrödinger equation (see below), is integrable and therefore pleasant from a mathematical point of view, real-world systems tend to be messy and are certainly not integrable. For many years loss (and gain) have mostly been treated as perturbations (see, e.g., Refs. [6–11]), which is applicable only to small perturbations. We have recently described how loss of arbitrary strength can be treated up to and including the assessment of soliton annihilation [12]; and meanwhile we have generalized this approach to amplifying fibers, including the generation of new solitons [13].

An alternative approach to increased efficiency of data transmission in a nonlinear channel was originally suggested by Hasegawa and Nyu [14]. Based on the observation that solitonic eigenvalues of the inverse scattering transform are more robust than pulse shape parameters under various perturbations, they suggested using the eigenvalues to code information. The suggestion lay almost dormant for about 20 years but has seen an enormous growth of attention recently [15–22]. The use of both the discrete and the continuous part [15,22] of the eigenvalue spectrum have been discussed, and estimates for achievable spectral efficiencies have been given [19]. In Ref. [19] propagation loss was considered to be compensated by Raman gain (and effectively traded for noise in the process).

We must point out, though, that very recently several authors have studied this topic [23–28] under aspects of the combined use of the continuous and discrete part [28] as well as polarization multiplexing [25,27] and some adverse effects [24]. Encouraging results have been obtained; in the experiments reported in Refs. [23,27] in particular, fiber attenuation and subsequent amplification were explicitly mentioned.

In the wider context of the fate of the eigenvalue spectrum outside the integrable limit, we here present a study specifically of the impact of loss. We concentrate on the discrete eigenvalue spectrum, because using the continuous part carries limitations on signal power and resembles more an analog system. The specific advantages of digital (but not necessarily binary) systems can only be had from the discrete spectrum (but see Ref. [28] for further discussion).

The discrete spectrum is trivial for a single soliton, and so we consider cases of more than one, starting with the well-known case of the $N = 2$ soliton, which has two discrete eigenvalues. It was pointed out many years ago that the two constituting solitons have zero binding energy [29,30] and hence are easily perturbed, which renders them less useful for communication purposes. That argument, however, applies to the pulse shape (temporal and spectral) but not to their eigenvalue structure.

In this paper we pursue the following program: We subject the $N = 2$ soliton compound to loss in the form of a localized attenuation as it may occur, e.g., at a splice between fiber

―――――
[*]fedor.mitschke@uni-rostock.de

segments and check how the soliton content of the attenuated pulse, as gauged by its eigenvalues, is modified. Then we continue by considering some other states containing two discrete eigenvalues to see how far our conclusions may be generalized.

Several features encountered in the process have been reported before in places scattered across the literature. This includes shifting and splitting of solitonic eigenvalues in certain sets of circumstances. We will discuss these sources in Sec. V and clarify how we put those various observations into a coherent context.

II. BASIC FACTS

We reiterate some established analytical results [31–33] for the sake of self-containedness. In the nonlinear Schrödinger equation (NLSE) in dimensionless form [33]

$$iu_\xi + \tfrac{1}{2}u_{\tau\tau} + |u|^2 u = 0, \tag{1}$$

ξ is the spatial coordinate (propagation distance), and τ time in a reference frame moving with the group velocity that pertains to the optical carrier frequency; $u = u(\xi, \tau)$ is the field amplitude envelope.

Equation (1) is integrable, and solutions can be found with the technique known as inverse scattering theory [31]. This method characterizes pulses by an eigenvalue spectrum, where discrete eigenvalues stand for solitons, and a continuous part for linear radiation. A soliton eigenvalue $\lambda \in \mathbb{C}$ has a real part $\mathrm{Re}(\lambda)$ indicative of its relative velocity, and an imaginary part so that $4\mathrm{Im}(\lambda)$ is the energy of that soliton. By virtue of integrability, eigenvalues are preserved: neither their number nor their values can change. More recently, the inverse scattering technique has also been known as the nonlinear Fourier transform [17–21,29].

If centered in the comoving frame, the fundamental soliton solution takes the form

$$u(\xi, \tau) = \eta \, \mathrm{sech}\,(\eta\tau) \exp\left(i\frac{\eta^2}{2}\xi\right) \tag{2}$$

with the scaling parameter η signifying at once the pulse amplitude, the inverse pulse width, and one half of the soliton energy.

Let us consider an initial condition in the form of a sech pulse

$$u(0, \tau) = N\eta \, \mathrm{sech}\,(\eta\tau), \tag{3}$$

where $N \in \mathbb{R}$ is an amplitude scaling parameter. In the special cases when $N \in \mathbb{N}$ one has N pure solitons; otherwise there is also linear radiation. In particular, for $N = 2$ one has a compound known as the $N = 2$ soliton. It consists of a nonlinear superposition of two fundamental solitons; their energy ratio is $\eta_1/\eta_2 = 1/3$. The exponential factor in Eq. (2) then dictates that their rates of phase evolution are in a 1:9 ratio.

During propagation the phase difference will grow; it will complete one cycle of 2π (one beat period) after propagation distance $\xi_0 = \pi/(2\eta_1^2)$. In the normalized system the $N = 2$

soliton has the form

$$u(\xi, \tau) = \frac{\cosh(3\eta\tau) + 3\cosh(\eta\tau)\exp(i4\eta^2\xi)}{\cosh(4\eta\tau) + 4\cosh(2\eta\tau) + 3\cos(4\eta^2\xi)}$$

$$\times 4\eta \exp\left(i\frac{\eta^2}{2}\xi\right), \tag{4}$$

where η is again the scaling factor; the $N = 2$ soliton energy is $E = 8\eta$. At $\xi = 0$ and again at $\xi = \xi_0$ the temporal profile has a real-valued sech shape. At half period $\xi = \xi_0/2$, it is also real-valued but consists of a central peak with a symmetric pair of side lobes so that the temporal profile has two nulls at positions $\tau_0 = \pm 1.317/(2\eta)$ [the numerical factor is $i\,\mathrm{arccos}(2)$]. At the same point the spectrum consists of two lobes with the same relative phase, peaking at positions $\Omega_\mathrm{p} = \pm 1.504\,\eta$ and a central null.

III. AN $N = 2$ SOLITON WITH LOCALIZED LOSS

Changes in eigenvalues of the inverse scattering technique can occur only when integrability is violated, e.g., by loss— but then the entire concept of eigenvalues becomes questionable. We consider a lossless fiber into which we insert a localized loss at some specific point; beyond that the fiber is considered lossless again. In this way the system is piecewise integrable, and the effect of the loss is simply that of a scaling factor of the entire pulse shape (and spectrum). We will refer to the loss position as the splice position below because fiber splices present a prominent example of localized loss, even though sharp fiber bends and the like have a similar effect.

Consider an initial pulse as in Eq. (3) with $N = 2$ propagating over a full soliton period ξ_0. In Fig. 1(a) the evolution of its spectral amplitude $|\tilde{u}(\Omega)|$ is shown; we specifically point out its double-humped structure around the halfway point. We now systematically investigate the effect of loss by varying both its position and amount. The position is chosen in $0 \leqslant \xi \leqslant \xi_0$ (beyond would be redundant); the loss is written as a factor $0 \leqslant M \leqslant 1$ multiplying the amplitude (compare Ref. [13]; in Ref. [12] the energy was attenuated by Γ so that $M = \sqrt{\Gamma}$).

For each ξ we vary M and apply numerical the direct scattering transform [18] to calculate the soliton content of the resulting pulse $Mu(\xi, \tau)$. Its soliton content is shown in Fig. 1(b). As one would expect, there are parameter regions where the number of remaining solitons is two, one, or zero. The labels designate the number of discrete eigenvalues, and whether they are different in energy (e) or in velocity or, equivalently, in frequency (f). Here (2e) denotes two solitons with different energy, both with zero center frequency, while (2f) denotes two solitons of the same energy, with symmetrically detuned center frequencies. If there is only a (1e) we omit the (e); (0) means that no soliton exists.

For certain positions in Fig. 1(b) the relative energies of solitons and radiation are known analytically for different loss factors M: Trivially, at $M = 1$ there is the unperturbed $N = 2$ soliton for all ξ, and at $M = 0$ there is no light at all. Also, at both $\xi = 0$ and $\xi = \xi_0$ we know that $M = 3/4$ corresponds to $N = 3/2$, the boundary between the single-soliton and two-soliton regimes; $M = 1/4$ corresponds to $N = 1/2$, the boundary between single-soliton and no-soliton regimes; and
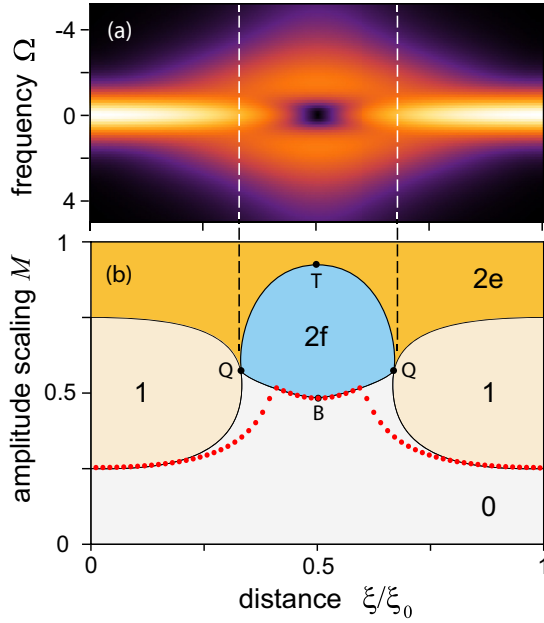
FIG. 1. (a) Evolution of the spectral amplitude $|\tilde{u}(\Omega)|$ of an $N = 2$ soliton over a whole soliton period ξ_0. Color indicates values form zero (black) to maximum (white). (b) Corresponding soliton regimes in the M-ξ plane for attenuation of amplitudes by M, localized at ξ. Labels indicate the number of solitons: "e" indicates energy splitting and "f" frequency splitting. The 2f regime is bounded by points T = (1/2, 0.922) (top), B = (1/2, 0.485) (bottom), and Q = $(1/2 \pm 0.170, 0.584)$ (quadruple points). Red dots mark predictions of a lower soliton threshold $M_{\min}$; see at the end of Sec. III. Vertical dashed lines mark regime of frequency splitting; see Sec. VI.

$M = 1/2$ corresponds to $N = 1$, the locus of the pure single soliton. All these features are clearly confirmed in Fig. 1(b). At positions other than ξ/ξ_0 integer, the pulse is not sech shaped, and distinct features arise.

We therefore compare the eigenvalues from the numerical direct scattering transform (representing soliton energy and frequency) for two splice locations, at $\xi = 0$ and at $\xi = \xi_0/2$ for various M; see Fig. 2. For $\xi = 0$ (left column) data show the well-known linear trend [32]: As M is increased, the first soliton appears at $M = 1/4$, the second at $M = 3/4$, while all frequencies remain at zero. All this, and the linear energy growth in particular, is as expected [32].

If the splice occurs at $\xi = \xi_0/2$ (right column), the situation is quite different: The threshold for solitons is at $M \approx 0.485$, but here a pair of solitons, split symmetrically in frequency with $\Omega_0 = \pm 1.54$, is born. Increasing M and thus amplitudes and powers, at $M \approx 0.922$ the frequencies coalesce, and the energies split. For $M \to 1$ the familiar energy values of $E_{N=1}$ and $3 E_{N=1}$ with $E_{N=1} = 2\eta$ are approached.

This is a remarkable qualitative change: A mere attenuation transforms two solitons of zero velocity into a pair with degenerate energy but different center frequencies. For $0.485 \leqslant M \leqslant 0.922$ the attenuated pulse contains two solitons with different velocities; upon further propagation it splits up in the time domain into distinct solitons and some radiation. In other words, a localized two-soliton structure does not persist. The bifurcation between two frequency-degenerate and two

energy-degenerate solitons thus marks the transition point between a sustained and a destroyed localized two-soliton structure.

To complete considerations of the bifurcation we preselected M and varied the splice position over the span of $0 \leqslant \xi \leqslant \xi_0$; see Fig. 3. We find that at half span the "stronger" soliton is attenuated while the "weaker" one receives a boost. At the bifurcation point at $M \approx 0.922$ both traces meet at a common energy value of $\approx 1.688 E_{N=1}$; this is the bifurcation point alluded to above.

FIG. 2. Soliton eigenvalues when the splice position is at $\xi = 0$ (left column) or at $\xi = \xi_0/2$ (right column). Upper row, energies in units of $E_{N=1}$; lower row, normalized frequencies.
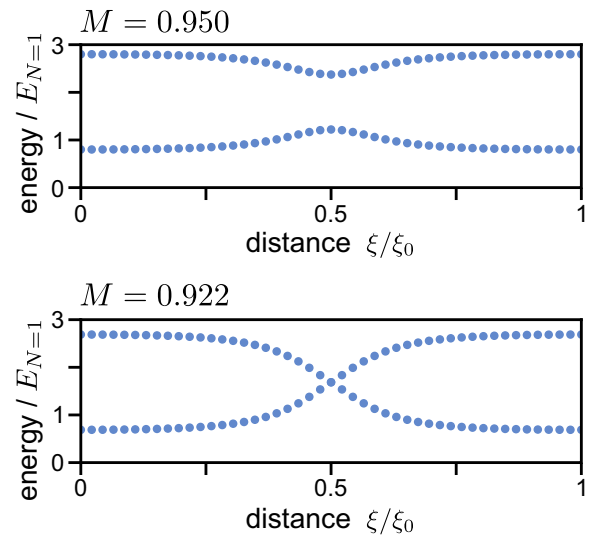
FIG. 3. Soliton energies when M is constant and the splice position ξ is varied. The lower-energy soliton peaks at 1.240 $E_{N=1}$ ($M = 0.950$) and at 1.688 $E_{N=1}$ ($M = 0.922$).
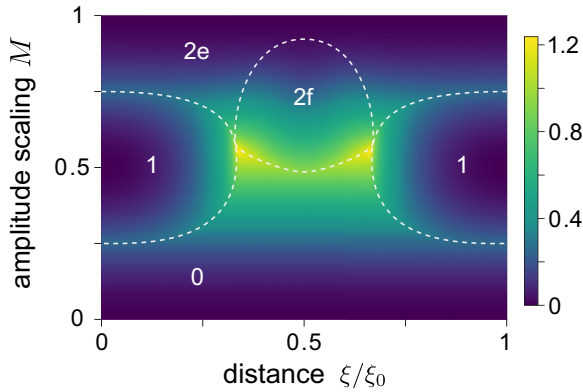
FIG. 4. Energy budget for the $N = 2$ case with localized loss; compare to Fig. 1(b). Shown is the radiation energy in units of the $N = 1$ soliton energy.

FIG. 5. Propagation of an in-phase double soliton amplitude $|u(\tau)|$ with an included local loss at $\xi = 0$. Three solitons are formed after loss: a blue-shifted soliton S_{bl}, a red-shifted soliton S_{rd}, and the most powerful center soliton S_{c}. Parameters of the initial soliton pair: $\eta = 1$, $\sigma = 8$; loss: $M = 0.6$.

These results may be wrapped up as follows: When an $N = 2$ soliton—a two-soliton compound—is attenuated, there may be two, one, or zero solitons left depending on the amount of loss. At the same time, some of the energy is converted into linear radiation. In the regime where two solitons survive there is a highly counterintuitive finding: The weaker soliton can receive a *net enhancement* of energy at the expense of the other, and that is no small effect: At $M = 0.922$, the overall energy loss is $1 - M^2 \approx 15\%$, but the energy of the weaker soliton grows by $\approx 69\%$. This peculiar result warrants a closer look into the energy budget. Figure 4 color-codes the parameter map of Fig. 1(b) to reveal the partition of energy to radiation. The analytically known cases at $\xi = 0$ are reproduced: 100% of the pulse energy resides in two solitons for $M = 1$, and in a single soliton at $M = 0.5$; in these positions the radiation vanishes. Radiation takes maxima at $M = 1/4$ and $M = 3/4$.

For $\xi \neq 0$, radiation is most prominent near the lower edge of the (2f) regime. In absolute terms, the maximum occurs near the "quadruple points" where the regions (2e), (2f), (1), and (0) meet at $\xi/\xi_0 = 0.5 \pm 0.170$.

If one of the quadruple points is horizontally transected by shifting the splice position ξ, a single soliton is rendered into a pair of frequency-split solitons. This is quite peculiar.

As a final sanity check, we discuss the lower threshold of M_{min} for any soliton to exist. We make use of the fact that there is a characteristic value of the peak spectral amplitude for any fundamental soliton, $\widetilde{u}_{\mathrm{sol,p}} = \pi$ (see the Appendix). M_{min} can then be found by attenuating the spectrum until its peak $\widetilde{u}_{\mathrm{p}}(\xi, \Omega)$ is reduced to one half of that characteristic value. This leads to $M_{\mathrm{min}} = \pi(2\widetilde{u}_{\mathrm{p}})^{-1}$. Note, however, that this is only a lower bound because if some radiation is also created, the energy requirement must be higher. As this prediction for M_{min} in Fig. 1(b) (red dots) shows, the general trend is reproduced very well, but there is a deviation precisely where radiative energy is maximal, i.e., near the quadruple points **Q**.

IV. EIGENVALUE SPLITTING OF TEMPORALLY AND SPECTRALLY SHIFTED SOLITON COMPOUNDS

As shown above, power loss alters the eigenvalues of an $N = 2$ soliton well beyond quantitative correction: it
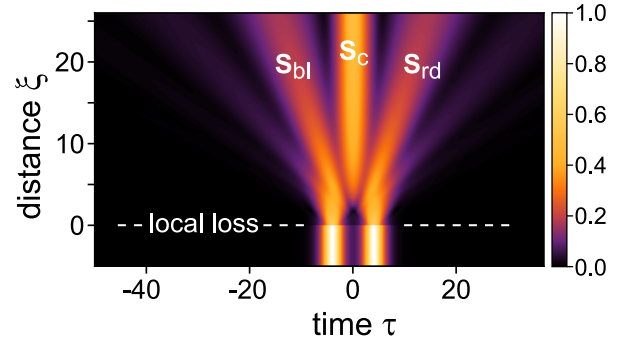
profoundly changes the nature of the eigenvalue spectrum. We will now proceed to discuss other two-soliton compounds to show that the qualitative modification is a general feature. It will emerge that whenever frequency splitting arises, we consistently see that the spectral shape of the soliton compound displays isolated humps. We argue that these seed the splitting process.

A. Copropagating solitons

The more pulses are attenuated, the more does their propagation resemble linear (dispersive) propagation. In Fig. 5 we show, as an example, a numerical simulation of the propagation of two sech pulses with identical parameters which are temporally separated by σ as in

$$u(\tau) = \eta \, \mathrm{sech} \, [\eta(\tau - \sigma/2)]$$
$$+ \eta \, \mathrm{sech} \, [\eta(\tau + \sigma/2)] \exp[i\varphi]. \quad (5)$$

We use $\sigma = 8$ and $\varphi = 0$ (in-phase pulses). At the marked position ($\xi = 0$) a loss with $M = 0.6$ is inserted. Thereafter, both pulses broaden, and once they develop sufficient overlap, an interference pattern appears. Each hump of that pattern can form an individual soliton under circumstances to be discussed now.

The Fourier spectrum of the pair of equal sech pulses has an overall sech-shaped envelope; underneath it there is a fringe pattern with spacing $2\pi/\sigma$ so that each fringe has a half width of about π/σ. Given that each fundamental soliton requires the same characteristic peak spectral amplitude $\widetilde{u}_{\mathrm{sol,p}}$ (see the Appendix), we need to assess the spectral power in each fringe in comparison to this characteristic value. As power is raised, more and more fringes will reach the characteristic value in the process.

As details also depend on their relative phases, we consider the cases of in-phase and opposite-phase pulses. In the former case, the spectrum will always have a central maximum, in the latter, a central zero, and in either case fringe positions and spectral amplitudes are symmetric. We illustrate this and the successive generation of solitons and soliton pairs in Fig. 6. It
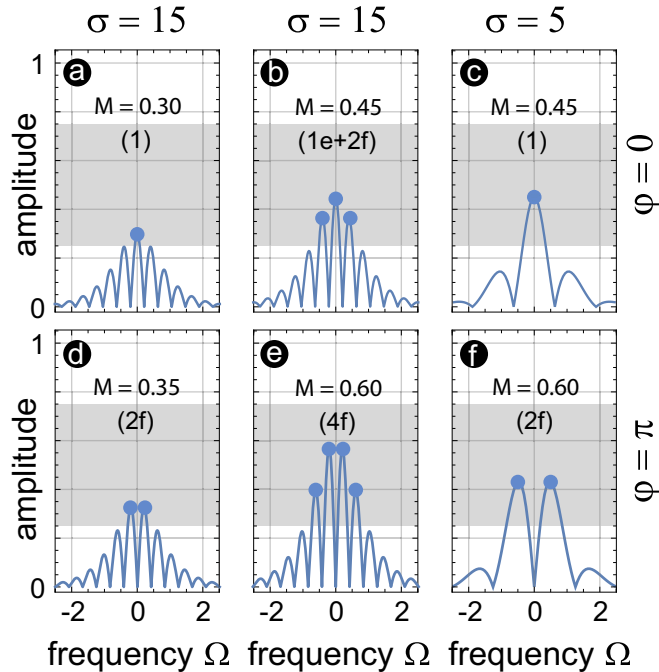
FIG. 6. Spectral amplitudes $|\tilde{u}(\Omega)|$ of two copropagating sech pulses with different separations σ and relative phases φ, normalized to twice the value of a single soliton as specified in the Appendix. Spectral fringes above the soliton threshold (gray region) correspond to individual solitons (marked by blue dots). The soliton content is given in the form $(x \cdot e + y \cdot f)$ with x solitons at center frequency and y frequency-split solitons with same energy. The spectral shape is crucial for the soliton content.

shows the spectral fringes of the double pulse from Eq. (5) for various constellations, in-phase ($\varphi = 0$) and opposite-phase ($\varphi = \pi$), wide ($\sigma = 15$), and narrow ($\sigma = 5$) separation.

The largest possible spectral amplitude $\tilde{u}_{\max}$, for fully constructive interference and zero relative velocity, is twice that of the fundamental soliton. Then for generation of a soliton each pulse must have a spectral amplitude of at least $\tilde{u}_{\max}/4$. For an in-phase pulse pair, the largest spectral peak is the one at center; it will reach threshold first [Fig. 6(a), marked by a dot]. The same argument then applies to the first pair of spectral "sidebands," i.e., the fringes next to the center: once they exceed threshold, a pair of new solitons will appear which are equal in all properties except their center frequencies which are $\pm 2\pi/\sigma$ [Fig. 6(b), pair of dots]. This reflects the splitting of the eigenvalues so that there are symmetric real parts. As a consequence, these solitons have velocities away from center, like in Fig. 5. The same logic is then repeated for further pairs of sidebands, giving rise to further pairs of frequency-split solitons. In Fig. 6(c) the temporal separation is reduced, which lets the spectral sidebands become wider and move outward. Then, fewer fringes under the spectral envelope remain above the power threshold.

For an opposite-phase pulse pair, the argument is similar except that there is no central peak. We therefore expect again that pairs of frequency-split solitons arise, with the sole distinction that the first soliton of the sequence, corresponding to a purely imaginary eigenvalue, does not materialize [Figs. 6(d)–6(f)].
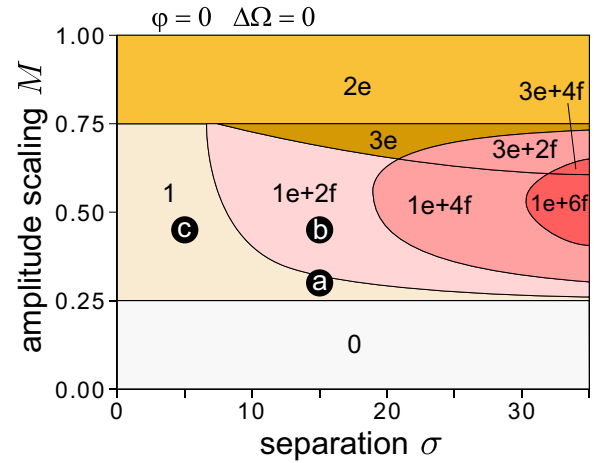
FIG. 7. Soliton content of two copropagating sech-pulses with relative phase $\varphi = 0$ depending on the separation σ and the amplitude scaling M. Below $M = 1/4$ there are no solitons; above $M = 3/4$ there are always two energy-split solitons. In between the content depends on the spectral fringes above the soliton threshold. Labels in black circles identify parameters for corresponding examples in Fig. 6.

Upon further increase of power, another threshold value occurs when the spectral amplitude reaches $3\tilde{u}_{\max}/4$. Once it is exceeded (for any of the humps), we expect a two-soliton compound. We will call the region between the two thresholds, i.e., $1/4 \leqslant M \leqslant 3/4$ the splitting regime; it is indicated by shading. Below, the number of solitons is zero; above, there are two with different energies (two imaginary eigenvalues). Humps that form solitons are marked by dots. Codes for soliton numbers are as above; e.g., (1e+2f) stands for one soliton at center frequency and two frequency-shifted solitons (one pair). Inside the splitting region, with increasing separation soliton compounds are therefore generated sequentially as (1), (1e+2f), (1e+4f), ...

If we consider in-phase pulse pairs, their spectrum will have equal-amplitude in-phase sidelobe pairs. This resembles the situation of an $N = 2$ soliton which around $\xi = \xi_0/2$ also has two symmetric spectral sidelobes. In the splitting regime, raising M can render a frequency-split soliton pair into an energy-split soliton pair. Figure 7 illustrates the eigenvalue content as a function of the scaling parameter and the separation. Data were obtained by direct scattering transform [18] as above. Here (1e+4f) can be converted to (3e+2f) by moving upward in the figure.

If, however, we start with opposite-phase pulse pairs, the spectrum has a central null, and symmetric pairs of humps are in opposite phase to each other. In this situation no energy-split pairs, but only frequency-shifted soliton pairs, can be generated. Consequently, Fig. 8 shows regimes of (2f), (4f), (6f), etc., when the separation is increased. At very small separation, destructive interference precludes the formation of any soliton.

B. Solitons with relative velocities

Adjacent channels in wavelength division multiplexing have different dispersion, and thus interchannel collisions
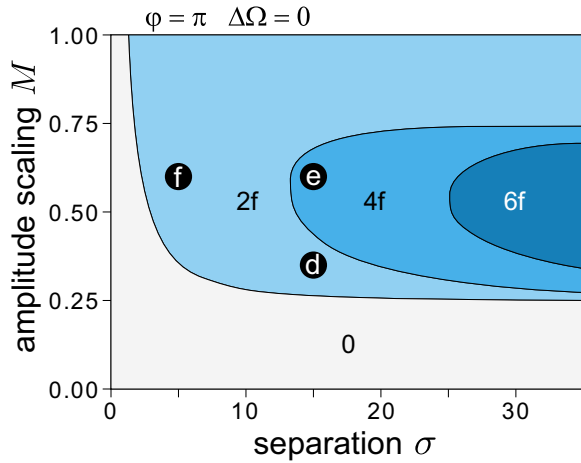
FIG. 8. Soliton content of two copropagating out-of-phase sech-pulses. Plot style corresponding to Fig. 7. Only frequency-split soliton pairs exist. Below $M = 1/4$ there are no solitons; above $M = 3/4$ and $\sigma = 2$ there are always two frequency-split solitons. Labels in black circles identify parameters for corresponding examples in Fig. 6.

FIG. 9. Soliton content of an in-phase pair of pulses at a relative velocity of $\Delta\Omega = 0.5$. The splitting region is reduced to ca. $0.38 \leqslant M \leqslant 0.63$. In this regime, a central soliton is always present, while with increasing σ more and more frequency-split soliton pairs appear. For more details see text.

occur at some relative velocity defined by $\Delta\Omega$. The temporal field of two frequency-shifted sech pulses is constructed by

$$u(\tau) = \eta \operatorname{sech}\left[\eta\left(\tau - \frac{\sigma}{2}\right)\right]\exp\left[-i\Delta\Omega\left(\tau - \frac{\sigma}{2}\right)\right]$$
$$+ \eta \operatorname{sech}\left[\eta\left(\tau + \frac{\sigma}{2}\right)\right]\exp\left[i\Delta\Omega\left(\tau + \frac{\sigma}{2}\right) + i\varphi\right]. \tag{6}$$

The velocity precludes full modulation contrast of the spectral fringes and can introduce spectral chirp to the individual fringes. Then the threshold for soliton generation at $\widetilde{u}_{\max}/4$ discussed above does no longer apply: the threshold is raised. In contrast, the upper threshold for single soliton generation at $3\widetilde{u}_{\max}/4$ is lowered: consider well-separated spectra; then for each the threshold becomes $\widetilde{u}_{\max}/2$. All told, the splitting regime shrinks from both sides. Below it, there are no solitons; above, there is always a frequency-split pair (2f) due to the initial frequency shift of colliding solitons.

For opposite-phase pulses the situation is not much different from that shown in Fig. 8 except that the vertical extent of the (4f), (6f) regimes is reduced. For in-phase pulse pairs, however, the situation is more complex. An example for moderate relative velocity is shown in Fig. 9. On the one hand, in the core-splitting region at $M \approx (0.5 \pm 0.1)$ the soliton content is comparable to the case of copropagating solitons as shown in Fig. 7 with a central frequency soliton and additional frequency split soliton pairs. On the other hand, velocity affects the spectral amplitudes; taking also spectral chirp into account, it can happen that a pair of side lobes becomes solitonic before the central lobe does. Then a frequency-split soliton pair appears first, before any soliton at center frequency. This explains the narrow stripe of (2f) near $\sigma = 15$, $M = 0.38$. At large M there is a closed (2f) region due to the relative velocity in contrast to a (2e) region of copropagating solitons.

Figure 10 shows what happens when the relative velocity is increased even more. The splitting region is further narrowed
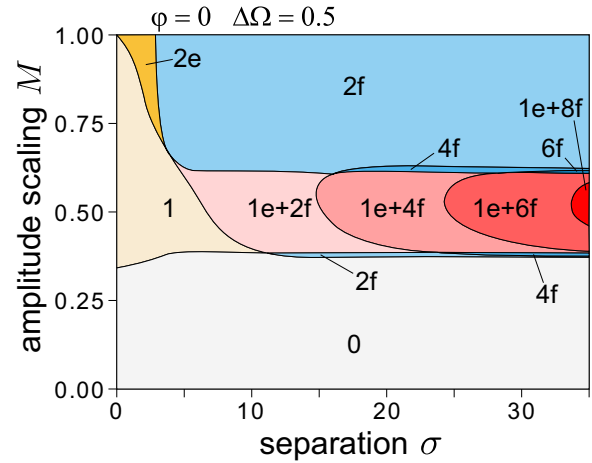
from above and below. The central soliton disappears first; this is due to the increasing spectral chirp of the central spectral fringe. Then the remaining frequency-split soliton pairs survive only in "islands" each of which shrinks when the velocity is further increased, until they eventually vanish. Note that the border between (0) and (2f) regions undulates with periodicity $2\pi/(\Delta\Omega)$; this is due to temporal fringes induced through the relative motion. For $\Delta\Omega \gg 1$, the border at $M = 1/2$ marks the transition between no-soliton and two-soliton (2f) regimes.
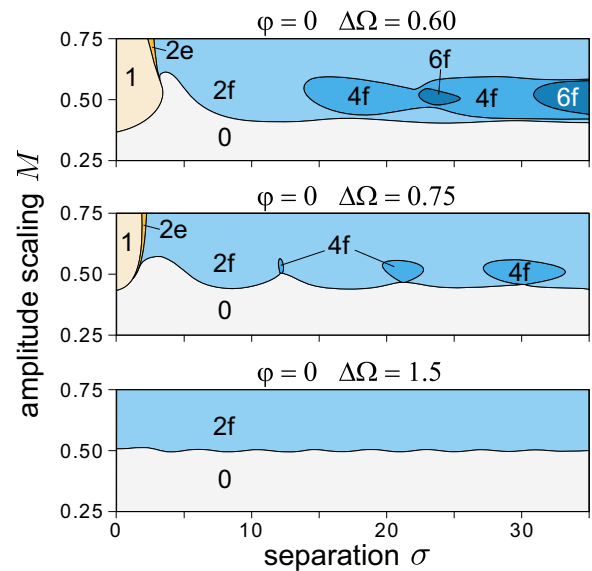
FIG. 10. Soliton content of in-phase pairs of pulses at relative velocities of $\Delta\Omega = 0.60$, 0.75 and 1.5. With increasing velocity the splitting region (see Fig. 9) narrows, leaving islands of frequency-split soliton pairs. The islands themselves shrink and eventually disappear with growing velocity, as set by $\Delta\Omega$.

V. COMPARISON TO LITERATURE

A. Pulses and soliton number

In one of the first studies of higher-order soliton, Satsuma and Yajima [32] solved the initial value problem for the hyperbolic-secant shaped pulse. They showed that with increasing amplitude the pulse contains a growing number of solitons, each with a purely imaginary eigenvalue. This is a general rule not just for sech-shaped pulses [34]. In a pulse there may be linear radiation which corresponds to a continuous part of the eigenvalue spectrum; together with solitonic energies it completes the energy budget of the pulse. As the NLSE is integrable, conservation of all eigenvalues is guaranteed.

A pulse containing a soliton and no radiation is called a pure soliton; it has a flat phase. Comparing to a pulse of the same envelope but with a chirp, the latter will contain some radiation and thus has less energy for the solitonic part [35–37]. It follows for pulses with more than one soliton that, if one considers increasing chirp, the soliton count will be reduced. This was first pointed out in Ref. [35], and later studied in Ref. [38] for a somewhat artificial simplified situation, and in Ref. [39].

B. Imaginary eigenvalues can move up and down

Introduction of a loss term into the NLSE lifts integrability, and eigenvalues are no longer preserved: the soliton content may change *during propagation*. Loss leads to changes of both the number of eigenvalues and their numerical values. This has mostly been considered for distributed (continuous) loss, see Refs. [15,40–42], but in Ref. [30] an asymmetrically tuned spectral filter was considered.

One might naively expect that when a pulse containing several solitons is attenuated, all solitons will undergo a proportional attenuation. This is not what one observes. Reference [32] shows that eigenvalues can all decrease at the same absolute rate, but even that turns out to be a special case. In general, one finds that during attenuation, some of the eigenvalues actually can *gain* energy at the cost of the others, as reported, e.g., in Refs. [35,39,42–44]. We have here quantified this phenomenon to show that the paradoxical enhancement of the weaker soliton by attenuation is no small effect.

C. Imaginary eigenvalues can collide and then have a real part

In an integrable situation, conservation of eigenvalues dictates that chirp can provoke frequency components to split only when this splitting exists in the initial condition in the form of eigenvalues with real parts. Indeed, in Ref. [39] "for certain phase functions and chirp strengths" such splitting is observed, but "another scenario is also possible" where the soliton content vanishes entirely. Similar eigenvalue splitting was found for single pulses with nonlinear temporal phases [35,38,39] as well as for real-valued signals with more than one temporal hump [43–45]. The same logic is applicable to spatial solitons [46].

In the presence of loss, eigenvalues evolve during propagation, so that imaginary eigenvalues approach each other and eventually collide. Beyond the collision point they acquire

real parts, one of which mirrors the other; this corresponds to a symmetrical frequency splitting. In Ref. [42] the splitting point is found in the limit of weak loss by a perturbation method, but it is stated that "in the case of strong nonadiabatic loss the evolution of the Zakharov-Shabat eigenvalues can be quite nontrivial." In Ref. [44] a simplified situation (double box potential) was considered, and the same kind of frequency splitting was reported.

Our observation of frequency splitting seems to be connected to the spectral shape of some signal: eigenvalues with nonzero velocities can be connected to distinct humps in the optical spectrum. They may appear as soon as the spectral lobes are lifted above the critical value (see the Appendix), which can happen due to amplitude scaling or, e.g., due to the variation of pulse separation. When the spectrum is symmetrical, these solitons emerge as soliton pairs. We checked our observations for the examples shown in Refs. [35,38,39,45–47] and find quantitative agreement with our theory.

VI. DISCUSSION AND CONCLUSIONS

As it is difficult to treat continuous loss beyond the perturbation regime, we decided to consider localized loss. This invokes one more parameter: beyond the cumulated loss amount over fiber length, there is also the position at which the loss occurs. However, this kind of treatment has the advantage that the system is "piecewise integrable" so that it is accessible; also, the way loss affects the pulse when applied at different positions allows additional insight.

We have first looked into a well-known example, the $N = 2$ soliton. Our results show that the same energy loss may or may not lead to frequency splitting, depending on the location within the soliton period where it acts. Obviously the evolution, which is periodic with ξ_0, affects parameters that are decisive.

The unchirped sech pulse shape at integer ξ/ξ_0 is favorable for conversion of the energy *of the attenuated pulse* into a new soliton (or new solitons): As little as 1/16 (6.25%) of the initial energy suffices to create a soliton, whereas at half-integer ξ/ξ_0, $\approx 85\%$ of the initial energy must be retained to create a soliton pair. In the entire range $\xi = (0.500 \pm 0.170)\xi_0$ (between the quadruple points) there is no obvious way to generate a single soliton. And we point out a remarkable coincidence: The beating between its two fundamental solitons leads to spectral side lobes in a section of the propagation distance, marked in Fig. 1 by the vertical dashed lines across Fig. 1(a) and Fig. 1(b). At the same time these markers are delimiters for the regime of frequency splitting (between the quadruple points). This demonstrates that a frequency-split pair is created if and only if the power is lowered (by a sufficient amount) where the spectrum is not single-lobed. We argue that this is not the case in this example alone but constitutes a general rule.

Various circumstances can cause the spectrum of a pulse structure to develop two humps, symmetrically displaced from the center frequency by $\pm\Delta\Omega$. In a linear (purely dispersive) system, fields corresponding to these humps would subsequently move away temporally from the center with relative velocities of $\pm\Delta\Omega$. If there is sufficient nonlinearity (i.e., sufficient power level), however, the opposite may happen:

Both lobes are pulled into place and remain as part of a compound structure.

In other words, nonlinearity can thwart dispersive walk-off, just as it prevents dispersive spreading in a standard soliton. This is the explanation why below some threshold power a structure with side lobes turns into a structure with pulses walking off symmetrically. We identify the threshold as the point of equilibrium between dispersive and nonlinear effects.

We went on to show other examples of side lobe pairs created by interference between two solitons, either with or without initial relative velocity. The former case is relevant for considerations of eigenvalue communication, the latter becomes relevant when wavelength division multiplexing is taken into consideration. Again a frequency-split pair walks off when the power level is reduced below a certain threshold. Several observations reported in the literature about soliton behavior in the presence of loss were thus put into a unified context.

There is an interesting connection to the "single lobe theorem" by Klaus and Shaw [34], which states the following: If the temporal pulse shape is single-humped and real, eigenvalues are confined to purely imaginary values. This implies a negation: for pulse shapes that fail to be real, or to be single lobed, or both, there is a possibility of eigenvalues with nonzero real part, i.e., frequency splitting. A few examples for this were provided both by Klaus and Shaw [34,47] and, as discussed above, by other authors too [35,38,39,45,46].

We note that negation of the theorem's conditions usually implies multiple (two or more) humps in the spectrum. Nonreal shapes can have more-than-single-humped spectra; consider the chirped rectangular temporal shape described in Ref. [47]. Non-single-lobed temporal profiles correspond to non-single-lobed spectral profiles due to interference fringes. Our conclusion is that multiple (two or more) humps in the spectrum can give rise to frequency splitting, provided that a certain condition applies. We showed what that condition is: Dispersion and nonlinearity are antagonists; the bifurcation from energy-split to frequency-split eigenvalues occurs at the point of balance between both. Their relative strength in a given fiber (fixed dispersion coefficient) can be adjusted by tuning the power level, so that variation of attenuation allows to scan across the bifurcation point. In this sense our results complement the single lobe theorem.

Outlook

Future research will have to consider these conclusions. As concerns eigenvalue communication, we already pointed out above that we find use of the continuous part of the eigenvalue spectrum less attractive than use of the discrete part. For that case we find that even for just two such eigenvalues, mild loss can already lead to unexpected and certainly undesired consequences. We demonstrated that for an $N = 2$ soliton splitting occurs at $M = 0.922$ corresponding to an energy loss of 15% or -0.7 dB. This indicates that eigenvalue communication is particularly vulnerable to power loss, compared to individual solitons which survive a localized loss of -6 dB. It must be assumed, until further investigation, that with increasing number of eigenvalues involved such challenges will only become increasingly harder to address.

Real-world systems use optical gain to compensate the loss. The question is whether with restoration of energy, a restoration of eigenvalues is also obtained. This is certainly the case for localized loss and gain when they are back to back, but with increasing distance between both the phase evolution in between will reduce the fidelity of restoration. With distributed loss there is always some distance involved, and a full restoration appears to be not possible. We have preliminary data indicating that in situations with two discrete eigenvalues as discussed in Refs. [23,27], the phase between the two solitons also has a large impact on the quality of restoration. In the worst case a frequency splitting by loss as described here cannot be undone by subsequent gain, and a severe transmission error occurs. The complexity of the situation will require further research, to find guidance in designing future experiments so that such problems hopefully can be safely avoided.

As concerns wavelength division multiplexed formats, the necessity to avoid eigenvalue splitting by interchannel interaction is one more good reason to keep WDM channels spectrally well separated. But even in single channel, to avoid collisions by intrachannel interaction confirms the need for sufficient temporal separation. None of this is favorable in terms of spectral efficiency and data rate.

A quarter century after the first proposal [14] it is not yet clear whether an eigenvalue-based transmission scheme can outperform the established transmission techniques but ongoing research is encouraging.

APPENDIX

It is a little noted phenomenon that all solitons in a given fiber, regardless of their scaling, have the same peak value of their spectral energy density. The peak amplitude is η, the peak power is η^2, the inverse duration is also η. The energy then is $E = 2\eta$. According to the power theorem of Fourier transform (a.k.a. Parseval's theorem; see, e.g., Ref. [48]), the spectral energy must be 2η, but the natural spectral width is $\Omega_0 = 2\eta/\pi$. The peak of the spectral amplitude $\widetilde{u}_{\mathrm{sol,p}} = \pi$ is therefore fixed, and the pertaining spectral energy density equals π^2.

In real world units, the familiar scaling of peak power and energy of a fundamental soliton with its natural temporal width T_0 is like $\hat{P} \propto T_0^{-2}$ and $E \propto T_0^{-1}$. In the Fourier domain, the natural width of the spectrum scales as $\omega_0 = 2/(\pi T_0)$. Then the spectral energy density at peak is independent of T_0 and is indeed given by $\widetilde{P} = \pi^2 |\beta_2|/\gamma$ with β_2 and γ being the group velocity dispersion parameter and nonlinearity parameter, respectively.

This means that in a given fiber, any soliton has the same characteristic value of spectral energy density, $\widetilde{P}$—a feature that can help identify them as it constitutes a necessary (but not sufficient in the presence of spectral chirp) condition.

[1] D. J. Richardson, Science **330**, 327 (2010).
[2] S. Murshid, B. Grossman, and P. Narakorn, Opt. Laser Technol. **40**, 1030 (2008).
[3] L. F. Mollenauer and J. P. Gordon, *Solitons in Optical Fibers: Fundamentals and Applications* (Academic Press, San Diego, 2006).
[4] P. Rohrmann, A. Hause, and F. Mitschke, Sci. Rep. **2**, 866 (2012).
[5] P. Rohrmann, A. Hause, and F. Mitschke, Phys. Rev. A **87**, 043834 (2013).
[6] A. Hasegawa and Y. Kodama, Proc. IEEE **69**, 1145 (1981).
[7] D. J. Kaup, SIAM J. Appl. Math. **31**, 121 (1976).
[8] V. I. Karpman and E. M. Maslov, Sov. Phys. JETP **46**, 281 (1977).
[9] Y. Kodama and A. Hasegawa, Opt. Lett. **7**, 339 (1982).
[10] K. J. Blow and N. J. Doran, Opt. Commun. **42**, 403 (1982).
[11] K. J. Blow and N. J. Doran, Opt. Commun. **52**, 367 (1985).
[12] F. Mitschke, A. Hause, and C. Mahnke, Phys. Rev. A **96**, 013826 (2017).
[13] C. Mahnke, A. Hause, and F. Mitschke, Intl. J. Opt. **2018**, 9452540 (2018).
[14] A. Hasegawa and T. Nyu, J. Lightwave Technol. **11**, 395 (1993).
[15] J. E. Prilepsky, S. A. Derevyanko, K. J. Blow, I. Gabitov, and S. K. Turitsyn, Phys. Rev. Lett. **113**, 013901 (2014).
[16] S. Hari, F. Kschischang, and M. Yousefi, in *27*th *Biennial Symposium on Communications (QBSC)* (IEEE, Kingston, ON, 2014), pp. 92–95.
[17] M. I. Yousefi and F. R. Kschischang, IEEE Trans. Inf. Theory **60**, 4312 (2014).
[18] M. I. Yousefi and F. R. Kschischang, IEEE Trans. Inf. Theory **60**, 4329 (2014).
[19] M. I. Yousefi and F. R. Kschischang, IEEE Trans. Inf. Theory **60**, 4346 (2014).
[20] M. Kamalian, J. E. Prilepski, S. T. Le, and S. K. Turitsyn, Opt. Express **24**, 18353 (2016).
[21] M. Kamalian, J. E. Prilepski, S. T. Le, and S. K. Turitsyn, Opt. Express **24**, 18370 (2016).
[22] E. G. Turitsyna and S. K. Turitsyn, Opt. Lett. **38**, 4186 (2013).
[23] V. Aref, H. Bülow, K. Schuh, and W. Idler, in 41st *European Conference on Optical Communications (ECOC)* (IEEE, Valencia, 2015), pp. 1–3.
[24] S. Civelli, E. Forestieri, and M. Secondini, IEEE Photonics Technol. Lett. **29**, 1332 (2017).
[25] J.-W. Goosens, M. I. Yousefi, Y. Jaouën, and H. Hafermann, Opt. Express **25**, 26437 (2017).
[26] S. T. Le, V. Aref, and H. Buelow, Nat. Photonics **11**, 570 (2017).
[27] S. Gaiarin, A. M. Perego, E. P. Da Silva, F. Da Ros, and D. Zibar, Optica **5**, 263 (2018).
[28] V. Aref, S. T. Le, and H. Bülow, J. Lightwave Technol. **36**, 1289 (2018).
[29] Y. Kodama and A. Hasegawa, IEEE J. Quantum Electron. **23**, 510 (1987).
[30] A. R. Friberg and K. W. DeLong, Opt. Lett. **17**, 979 (1992).
[31] V. E. Zakharov and A. B. Shabat, Sov. Phys. JETP **34**, 62 (1972).
[32] J. Satsuma and N. Yajima, Suppl. Prog. Theor. Phys. **55**, 284 (1974).
[33] G. P. Agrawal, *Nonlinear Fiber Optics*, 5th ed. (Academic Press, San Diego, 2013)
[34] M. Klaus and J. K. Shaw, Phys. Rev. E **65**, 036607 (2002).
[35] L. V. Hmurcik and D. J. Kaup, J. Opt. Soc. Am. **69**, 597 (1979).
[36] D. Anderson, M. Lisak, and T. Reichel, J. Opt. Soc. Am. B **5**, 207 (1988).
[37] C. Desem and P. I. Chu, Opt. Lett. **11**, 248 (1986).
[38] D. J. Kaup, J. El-Reedy, and B. A. Malomed, Phys. Rev. E **50**, 1635 (1994).
[39] M. Desaix, L. Helczynski, D. Anderson, and M. Lisak, Phys. Rev. E **65**, 056602 (2002).
[40] E. M. Dianov, Z. S. Nikonova, and V. N. Serkin, Sov. J. Quantum Electron. **16**, 219 (1986).
[41] Jaroslaw E. Prilepsky, Stanislav A. Derevyanko, and Sergei K. Turitsyn, JOSA B **24**, 1254 (2007).
[42] J. E. Prilepsky and S. A. Derevyanko, Phys. Rev. E **75**, 036616 (2007).
[43] M. Desaix, D. Anderson, L. Helczynski, and M. Lisak, Phys. Rev. Lett. **90**, 013901 (2003).
[44] E. N. Tsoy and F. K. Abdullaev, Phys. Rev. E **67**, 056610 (2003).
[45] M. Desaix, D. Anderson, and M. Lisak, Phys. Lett. A **372**, 2386 (2008).
[46] D. Burak, Phys. Rev. A **52**, 4054 (1995).
[47] M. Klaus and J. K. Shaw, Opt. Commun. **197**, 491 (2001).
[48] R. N. Bracewell, *The Fourier Transform and Its Applications* (McGraw Hill, New York, 2000).